UDC 621.396.96 **doi: 10.32620/reks.2024.4.11**

Volodymyr PAVLIKOV[1], Simeon ZHYLA[1], Pavlo POZDNIAKOV[2], Denys KOLESNIKOV[1], Hlib CHEREPNIN[1], Olexandr SHMATKO[1], Oleksii ODOKIIENKO[1], Pavlo MALASHTA[1], Eduard TSERNE[1]

[1] National Aerospace University "Kharkiv Aviation Institute", Kharkiv, Ukraine
[2] State Service of Special Communications and Information Protection of Ukraine, Kyiv, Ukraine

FOUNDATIONS OF RADAR SYNTHESIS THEORY OF PHANTOM OBJECTS FORMATION IN SAR IMAGES

The primary research area is developing a theory of false object formation in aerospace radar images. This process involves adding the spatial and temporal trajectory signals of the object information features that are absent on the underlying surface irradiated by an aerospace carrier. The ***goal*** *of this study is to determine the general concepts of the design and application of radar image phantomization radars. The research is aimed at solving the following* ***tasks****: to describe the general concept of phantomization radar (PhR) design and application; to formulate the hypotheses underlying the theory and outline the range of issues to be solved; to determine the general structure of PhR; to develop mathematical models of the laws of distance change in the system "phantom image generator – remote sensing radio system"; to determine the size limitations of the area where phantom replacement of real radio images can be provided following the viewing mode of the underlying surface from satellites. The solution to these tasks is based on the* ***methods*** *of the remote sensing system synthesis theory, radiophysics, coherent image formation, functional analysis, synthesis, and processing of spatiotemporal signals. The following* ***results*** *were obtained: 1) the structure of the PhR is defined, which includes a receiver, a bank of SAR signal models, a bank of object models to be injected into the PhR signal, and a transmitter; 2) the parameters of the received SAR sensing signal that need to be estimated in the PhR receiver are determined; 3) the geometry of interaction in the "SAR-PhR" system is described, which allowed us to determine an expression for estimating the distance between SAR and PhR, as well as to estimate the distance-related parameters, such as signal delay time and characteristics of sensing signals.* ***Conclusions****. This paper describes several primary issues that arise in the development of the phantomization radio image theory. The results obtained are the foundation for further research, which should be directed toward the development of mathematical models of the aerospace remote sensing system orbits, spatial and temporal signals emitted by the remote sensing radio systems from aerospace carriers, and formalization of the features of the underlying surface in the "SAR-PhR" system.*

Keywords: *remote sensing theory; radar imaging; SAR imaging; signal processing.*

1. Introduction

Motivation. Remote sensing systems [1, 2] equipped on aerospace carriers operating in the radio waveband have a prominent role in the overall structure of obtaining information about the Earth's surface. This is due to the following advantages: coverage of large areas of the underlying surface (a wide observation angle during flight at high altitudes provides a wide swath of view); real or quasi-real-time information acquisition; information can be obtained at any weather and regardless of the time of day, which is associated with the radio wave signal processing; and high spatial resolution comparable to the optical sensing systems' resolution, achieved by modern algorithms of spatiotemporal signal processing [3, 4]. Remote sensing systems make it possible to obtain radio images throughout the year, whereas optical images for many regions of the Earth are rarely available for more than one-third of the year due to atmospheric opacity (cloud cover).

For many tasks, remote sensing data on the underlying surface plays an important role, providing initial information about the state of the underlying surface. These are, first, research tasks related to agricultural fields, glaciers, forests, and water surfaces, and many others. Radio images are also used in reconnaissance tasks. In such cases, systems must be designed and developed to prevent the acquisition of reliable radio information in specific areas of the Earth's surface. This can be achieved by synthesizing radio signals with the necessary information about objects in a given area that are not there. Such signals, once processed in aerospace synthetic aperture radars, will result in the appearance of "phantom" objects on radio

ISSN 1814-4225 (print)
ISSN 2663-2012 (online)

images. Accordingly, the theory that describes the synthesis of radio engineering systems that will form these signals should be defined as radio image phantomization.

State of the Art. It should be noted that some work in this area is being carried out in all frequency bands used for remote sensing. For example, in optical and infrared bands, the issue of preventing the acquisition of reliable information can be solved by creating object "dummies" and placing them on the underlying surface. The majority of information is available on enemy deluding in the optical and hyperspectral optical ranges. In [5, 6], the authors presented the demasking features of military equipment on battlefields in real-time optical and hyperspectral wavebands. Studying these works allows us to identify the characteristics that should be implemented in target imitation objects. These characteristics create the illusion of real targets for automatic detection systems. Information about features (geometric, spectral, etc.) is also used in the design of technical objects, in particular, robots [7]. Along with the detection of characteristics in the optical range, the functionality of systems is often expanded in the infrared range. For example, [8] justified the possibility of increasing the detection probability of technical objects using hyperspectral data in the optical and infrared ranges simultaneously. In particular, it has been pointed out that such an expansion of the spectral range increases the probability of detecting complex targets at the subpixel level, making it possible to identify hidden objects, as well as chemicals in plumes, and even detect vehicles hidden under a small layer of soil. Once again, taking these features into account allows us to improve the quality of creating dummies for misleading purposes, which is ideologically related to the direction of the article but based on other physical principles of forming an "illusion". The radio range is no exception; thus, scientists pay considerable attention to studying the demasking (masking) characteristics of military vehicles. The simplest works deal with corner reflectors and their ordered systems. In [9], the energy characteristics necessary to determine the effectiveness of installing false targets in the form of corner reflectors were investigated by calculating the similarity of the range profile based on the curve intersection obtained by the cosine similarity method and the range profile deflection peaks. The calculations are based on the example of a corner reflector system used to form false targets at sea to imitate ships. In [10], the results of the radio signal polarization characteristics were scattered on a tank model, which is extremely important for proper masking of radio images. Article [11] presents the results of jamming synthetic aperture radars (SAR), which are the main ones used for aerospace imaging and allow the acquisition of radio images with spatial resolution comparable to optical resolution. This is based on the use of corner reflector systems, which, depending on the distance between them and the viewing angle, which varies depending on the relative position of the reflectors and the aerospace carrier (due to its orbit or a defined trajectory), will imitate the objects of various vehicles. If the corner reflectors are properly placed, the angle between them (the apparent distance) changes according to the viewing angle from the aerospace platform. This work and others similar to it do not pay attention to the idea of forming a signal to "replace" the radio image, which may become dominant in the coming decades, considering the rapid progress of the radio element base. The theory, the foundations of which are described in this paper, proposes a replacement signal for synthetic aperture radars. A distant relation to this idea is a simple time delay averaged from several reception points and an amplified satellite signal for inverse synthetic aperture radars [12]. This approach makes it possible to radiate a copy of the sensing signal from one place but does not create "phantoms" in a specific area.

In contrast, the proposed method assumes that a single phantomization system will cover a specific area with images of objects that are not currently present in a given area. This is extremely relevant considering the following. To obtain radio images of objects that do not currently exist in a given area, a system of corner reflectors (placed according to certain patterns) can be used. This approach is convenient to implement when simulating some objects. To create the "illusion" that numerous vehicles (or buildings) are located in specific areas, this approach requires several corner reflectors. In addition, this approach does not provide the "illusion" of vehicle movement/relocation in radio images. It creates a contradiction: on the one hand, there is a need to create systems to prevent obtaining true information by imitating a large number of objects (vehicles, structures, and buildings) in the radio range over large areas, and on the other hand, there is no theory of synthesis of methods and systems of image phantomization without physical objects-imitators. This contradiction raises the problem of developing a foundation for radio image phantomization theory at the level of forming false information injections into the signals of aerospace radiovision systems. The solution to this problem requires the development of an appropriate theory, which should be based on the current knowledge of the radiovision system design, radio image processing, radio physics (forward and inverse problems), estimation of spatiotemporal signal parameters, digital information processing, and machine vision. In particular, information from [13, 14] concerns modeling the formation of vehicle visual features on radio images. This information is important for developing the proposed theory; however, it is not fundamental. In general,

articles [9-14] indirectly contain information that points to the fundamental possibility of creating a theory of radio image phantomization.

Thus, the **object** and **subject** of the study are as follows. The research object is the process of injecting false objects (phantoms) into radio images generated by aerospace remote monitoring radio systems, in particular, synthetic aperture radars as a key radiovision system. The research subject is the development of a theory of false object formation in the images of aerospace radiovision systems by injecting the informational characteristics of objects not present on the irradiated surface into the spatiotemporal trajectory signals.

The article describes a wide range of primary issues that arise in the process of developing this theory: the general concept of PhR design and application is presented, the hypotheses underlying the theory are defined, the issues to be resolved are formulated, a generalized scheme of PhR is developed, and equations for the basic parameters and characteristics required for planning interaction sessions between PhR and SAR are derived.

The article is structured as follows. Section 2 formulates the main idea of phantomization theory, the working hypotheses that form its basis, and the main problems that arise in the process. Section 3 outlines the novelty of the proposed theory and the differences from existing solutions. In Section 4, the phantomization radar application geometry and the generalized design of such a radar are presented. Section 5 presents the mathematical formalization of the SAR signal, its transformation during transmission and reflection, and the received signal type. Section 6 presents the general structure of an onboard SAR in the context of a general application model. Section 7 focuses on determining the interaction time between the SAR and the phantomization radar for a circular satellite orbit. Calculating this time is important from the point of view because it is necessary to know in advance how long the PhR can interfere with the SAR operation. Section 8 presents the basic equation for the range between the SAR and the PhR, which determines the distance between these radars at any point in time. Section 9 provides calculations of the expected and maximum lengths of coherent pulse packets, which are usually used onboard satellite SAR. Section 10, considering the calculations in the previous sections, presents the synthesized radiation pattern depending on the sensing signal. Section 11 discusses the ideas and hypotheses put forward, the difficulties of forming the theory, the issue of optimal waveform determiner design, the existing limitations of parameters and waveforms, and the importance of calculating the complex scattering coefficient as a source of key information about the underlying surface. Section 12 concludes the paper by summarizing the PhR construction concept (i.e., the main elements of such a radar) and the geometry of the phantom radar application.

2. The Idea, Working Hypotheses, And Problems of Developing the Radio Image Phantomization Theory

Fig. 1 (borrowed from [15]) shows a radar image from Sentinel-1 distorted by the Russian jamming system for spaceborne synthetic aperture radars. Such distorted parts of radar images contain lost information that cannot be recovered by modern intelligent radio image filtering systems [16, 17].

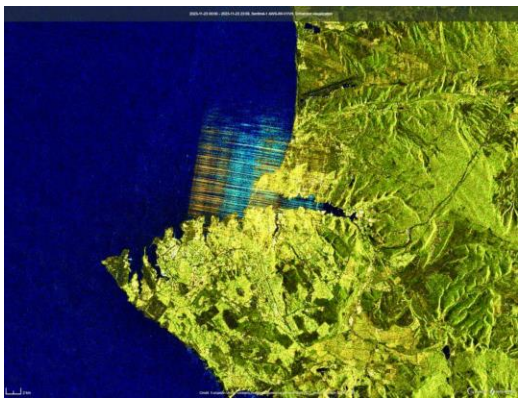

Fig. 1. Radar image at the synthetic aperture radar output (Sentinel-1 satellite) of a fragment of the temporarily occupied Crimean Peninsula, noised by radio jammer signals

The following **idea** arises: if a radio image can be distorted, it can also be edited (phantoms can be added) using information "injection" signals into the radio image. The proposed method can be implemented by injecting a signal with particular information characteristics into the true signal.

To implement this idea, we need a theory to develop which we propose the following hypotheses. **Hypothesis 1** – by adding a signal containing the necessary information characteristics to the signal of the radiovision system reflected by the underlying surface, it is possible to imitate the presence of objects with predetermined properties in places where they are not physically present or to increase their number where they are few. This approach is increasingly demanded because significant effects can be achieved by replacing information. **Hypothesis 2** – to develop the foundation of radio image phantomization theory, it is necessary to significantly develop knowledge in the following scientific areas: statistical theory of aerospace-based remote sensing radio systems; physics of radio wave interaction with various surfaces,

ISSN 1814-4225 (print)
ISSN 2663-2012 (online)

including radiophysics sensing of the Earth's atmosphere; radio navigation theory, etc. The complex vision of the radio image formation processes, radio wave emission and propagation (and their reflection), and processing of spatiotemporal signals in aerospace-based measurement and information radio systems allows us to understand and define the above problem. **Hypothesis 3**: the formation of an integral reflection signal that considers both the features of the real terrain and the objects included in it (with terrain reference) will allow one phantomization system for a particular surface area. **Hypothesis 4**: To create a lifelike effect of the object's presence, it is necessary to consider the mutual movement of the "satellite-radar" system in the process of phantomization signal formation, which requires knowledge of the satellite position in space and time, radiation signal form, parameters, and motion characteristics, etc. **Hypothesis 5** – all parameters and characteristics necessary for the system's functioning can be calculated or measured in advance by modern control and measuring equipment. These hypotheses form the foundation of the new theory.

Hypotheses 1-5 are based on a deep and integral understanding of radio image formation processes [18], and the experience of statistical synthesis of aerospace radio imaging systems [19, 20] leads to the conclusion that the idea is viable.

Creating a new radio image phantomization theory and developing recommendations for the design of corresponding radio systems requires solving the following tasks:

− development of the fundamentals of radio engineering systems theory, which replaces or adds radio images for aerospace remote sensing systems according to predefined scenarios;

− new components of the theory for estimating the parameters of signals emitted by aerospace remote sensing systems. These components of the theory include new mathematical models of signals considering the features of the expected orbit and motion parameters of the remote sensing radar, its operating modes, and the mutual movement of the "satellite-radar" system;

− new mathematical models of spatiotemporal trajectory radio signals containing information about the necessary elements – "phantoms") on the specified areas of the underlying surface. These models consider the features of signal backscattering by objects of different nature and, possibly, digital area maps in the radio wave range, as well as new methods of adding "injection" signals to the trajectory signals formed by radiovision systems;

− adjustment of the mathematical model to reflect the atmosphere state and the polarization processing features of the sensing signals;

− recommendations for the application of the new theory in the engineering implementation of radars. Analysis of theory application limitations.

It should be noted that the novelty of the approach lies in the first proposed use of a synthesized spatiotemporal signal (a signal with an "injection" of objects that are allegedly present in a given area of space), which will bring additional information to the radio images formed by aerospace synthetic aperture radar (SAR). The same signal will be adaptive to changes in the mutual position of the SAR-Phantomization Radar (SAR-PhR) system, which is necessary for the correct formation of information about the "injected" objects in the trajectory signals generated by SAR. It is expected that such signals will be described by complex mathematical expressions, but modern systems based on field-programmable gate arrays (FPGA) are capable of processing big data in real-time.

The solution to the above problems should begin with the formation of a general concept of design and application of radio images phantomization radars, defining the geometry of the problem taking into account the movement of the remote sensing aerospace carrier and its mathematical analysis, developing mathematical models of the distance change laws in the system "phantomization radar – remote sensing radio system", defining limitations on the size of the area where phantom replacement of real radio images can be provided following the satellite observation mode.

These primary tasks form the basis for other tasks, namely:

− development of mathematical models for the orbits of aerospace remote sensing systems and formalization of the features of the underlying surface observations in the context of application in the "SAR-PhR" system;

− development of mathematical models for the spatiotemporal signals emitted by remote sensing radio systems from aerospace carriers, considering different observation modes;

− improved mathematical model of radio image formation in synthetic aperture radars;

− creating a model bank of radio wave scattering based on the underlying surface areas that are most typical for Ukraine;

− the creation of generalized models of radio wave backscattering by objects to be phantomized in radio images;

− the development of mathematical models for radio signals reflected by spatially distributed underlying surface areas that have the information characteristics of phantom objects;

− development of new methods for "injecting" signals into aerospace radar systems that allow guaranteed changes in the radio image;

– studying the dynamics of signal waveform changes considering mutual movements in the "SAR-PhR" system;

– study of the atmospheric impact and adjustment of the mathematical models obtained in solving the previous problems by considering the dynamics of the mutual movement of the "SAR-PhR";

– development of a statistical synthesis method for radio image phantomization system;

– the development of a generalized block diagram of the radio image phantomnation system;

– development of general recommendations for the design and construction of radio image phantomization systems;

– analysis of the theory's limitations.

3. Novelty of the Proposed Theory

There is no mention in the literature of an analog of the synthesis theory of phantomization radio systems. There are only reports on the use of mockups of objects that look different in different frequency ranges: in the optical and infrared ranges, these are physical objects [5, 6, 8] that are similar in their geometric characteristics to various vehicles; in the radio range, systems of corner reflectors [9, 10] and time-delayed reemission of recorded and averaged signals [11]. In other words, there is no information on the related ideas or theoretical parts of such radio systems.

The new theory makes it possible to build radars that can imitate the presence of objects/buildings in a specific location. In studies [5-11], the imitation objects were assumed to be placed in a position where they should be displayed on an optical, infrared, or radar map. Thus, as seen in the available works, the formation of the illusion of many objects requires a lot of physical objects and considerable time for placement. Unlike this, the proposed theory allows adding information to the radio image replacement signal in a way that it will contain as many objects as can be placed in a specific area of the terrain (justification of the area size requires the development of an appropriate methodology), but in any case, this is a time and material gain compared to the current state of the art.

It is expected that the proposed theory will allow us to form the illusion of the presence of not only stationary objects but also the presence of moving vehicles, which was previously impossible without the physical movement of objects. This can be achieved by adding additional modulation to the "injection" signals (not to be confused with the tasks [21] of modeling SAR signals).

The theory implies the adjustment of information (change of parameters) in the phantomization radar signal in accordance with the change in the mutual location of the "ground radar–onboard SAR" system.

4. The Concept of Design and Application of Radio Image Phantomization Radars

The concept (geometry) of the phantomization radar is illustrated in Fig. 2.

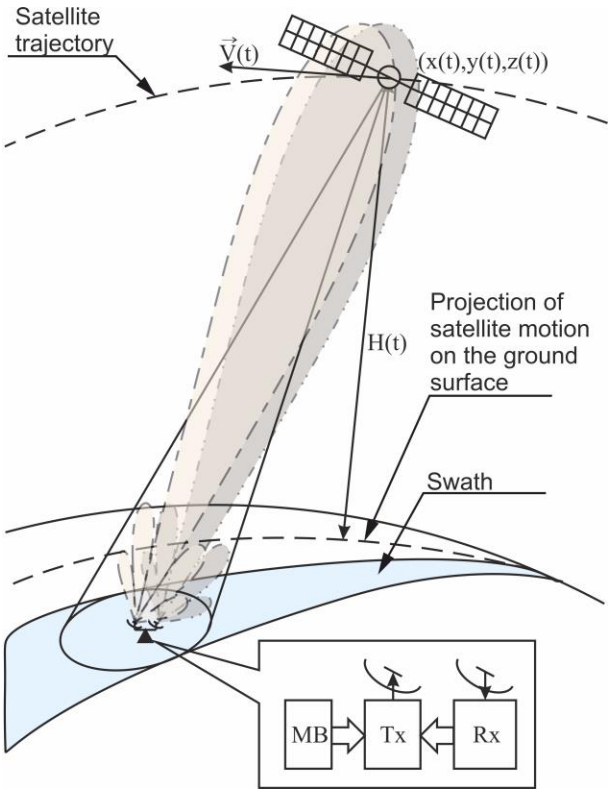

Fig. 2. General concept (geometry) of phantomization radar use

The concept of radar design:

1. The radar must contain three components (Fig. 2): a receiver (Rx); a transmitter (Tx); and a model bank (MB) of objects that are added to the transmitter signal.

2. The receiver solves the following tasks (depending on the operating mode):

– receiving satellite signals, amplifying them, and estimating their form and parameters;

– estimates the satellite flight parameters required for the system operation (records the fact of satellite appearance and the slant range to it);

3. The model bank contains a library of electrodynamic models of objects, which are recalculated into the transmitter signal parameters;

4. In the transmitter, based on the data received from the receiver regarding the form and parameters of satellite radar signals, satellite motion parameters, as well as data from the model bank, generate signals for the satellite that add object patterns to the radio image.

The transmitter and receiver antennas must be decoupled from each other. It is also assumed that the satellite-radar interaction session can be calculated in

ISSN 1814-4225 (print)
ISSN 2663-2012 (online)

advance, and in the best case, the form and estimates of the sensing signal parameters are already known and can be obtained from previous observations of remote sensing satellites. The transmitter and receiver can also be separated, and the receiver can operate separately for some time to create databases of SAR satellite signals.

Fig. 3 shows a generalized structure of interaction in the "SAR-PhR" system.

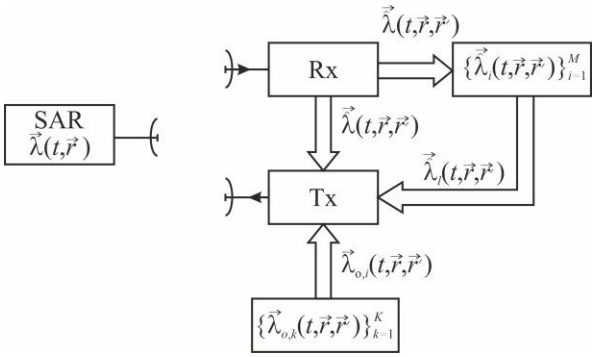

Fig. 3. Generalized block diagram of "SAR – PhR" system interaction

Fig. 3 contains the following abbreviations and notations:

– SAR – synthetic aperture radar (located on an aerospace carrier);

– $\vec{\lambda}(t,\vec{r}')$ is a vector of the true values of the signal form and parameters, and satellite motion parameters as a function of time t and spatial coordinates $\vec{r}'$ in the coordinate system related to the satellite;

– $\vec{\hat{\lambda}}(t,\vec{r},\vec{r}')$ is a vector of the estimates of the signal form and parameters, satellite motion parameters, as a function of time t and spatial coordinates $\vec{r}$ and $\vec{r}'$ in the coordinate systems related to the phantomization radar and the satellite, respectively;

– $\vec{\hat{\lambda}}_l(t,\vec{r},\vec{r}')$ is a vector of estimates of the form and parameters of the signal, and motion parameters of the 1st satellite, considering the position of the phantomization radar;

– $\left\{\vec{\hat{\lambda}}_i(t,\vec{r},\vec{r}')\right\}_{i=1}^{M}$ is a memory unit that stores information on the vectors of estimates of the form and parameters of signals, and motion parameters of the M-th satellite, considering the phantomization radar's position;

– $\vec{\lambda}_{o,i}(t,\vec{r},\vec{r}')$ is a vector of the object characteristics to be added to the signal parameters of the phantomization radar;

– $\left\{\vec{\lambda}_{o,k}(t,\vec{r},\vec{r}')\right\}_{k=1}^{K}$ is a bank of object characteristics to be added to the phantomization radar signal parameters.

If there is a priori information about the satellite's motion and SAR characteristics in the memory unit $\left\{\vec{\hat{\lambda}}_i(t,\vec{r},\vec{r}')\right\}_{i=1}^{M}$, it is advisable to use them, as shown by another arrow from the mentioned unit to the transmitter Tx.

5. General Form of the Onboard SAR Sensing Signal and Signal Transformation in the Process of Sensing

To solve the problem of radio image phantomization, it is important to describe the general form of the onboard SAR sensing signal and examine the transformation of this signal that occurs during the sensing process.

The onboard SAR sensing signal can be written in a very general form [22] as follows:

$$s(t) = \mathrm{Re}\left\{\dot{A}(t)\exp\left(j2\pi f_0 t\right)\right\}, \qquad (1)$$

where $\dot{A}(t)$ is the signal's complex envelope, which can describe various types of modulation and any form (from a pulse to a coherent packet of pulses), $\mathrm{Re}\{\cdot\}$ is the real part of the complex number, f_0 is the carrier frequency, and t is the time variable.

To write down the signal recorded by the SAR antenna on board an aerospace vehicle, we first write down a unit signal, i.e., the signal reflected by an elementary area of the underlying surface. To do this, we consider the geometry shown in Fig. 4.

Fig. 4 shows the antenna system of an onboard SAR, which is represented by the area D' with the phase center at pt. O'. The underlying surface S, which contains an elementary area dS, the distance to which from the phase center of pt. O' is denoted by $R_0(\vec{r},t)$. The complex scattering coefficient of the underlying surface is denoted by the function $\dot{F}(\vec{r},\vec{r}',\vec{\lambda}(\vec{r}))$, which depends on the coordinates of the underlying surface $\vec{r}$, the geometry of mutual placement in the "SAR–observation point" system, which is indicated by the dependence on the coordinates of $\vec{r}'$, the parameters of this surface $\vec{\lambda}(\vec{r})$, which can be estimated when solving remote sensing problems. The distance from the same elementary area to any area dD' of the antenna system is denoted by $R(\vec{r},\vec{r}',t)$. The $Oxyz$ coordinate system is related to the underlying surface. The plane xOy goes through the mean level of the underlying surface (the roughnesses in Fig. 4 are not shown, but they occur in the remote sensing

practice). Surface roughness can be introduced as an additional phase shift $\varphi(\vec{r},\vec{r}',\vec{\lambda}(\vec{r}))$ in the complex scattering coefficient $\dot{F}(\vec{r},\vec{r}',\vec{\lambda}(\vec{r})) = |\dot{F}(\vec{r},\vec{r}',\vec{\lambda}(\vec{r}))|\exp(j\varphi(\vec{r},\vec{r}',\vec{\lambda}(\vec{r})))$. The coordinate system $O'x'y'z$ is related to the phase center of the onboard SAR antenna system. The radius vectors $\vec{r}$ and $\vec{r}'$ describe the elementary areas' positions in the $Oxyz$ and $O'x'y'z$ coordinate systems, respectively (to simplify mathematical calculations, they can be assumed to be in the xOy and $x'O'y'$ planes).

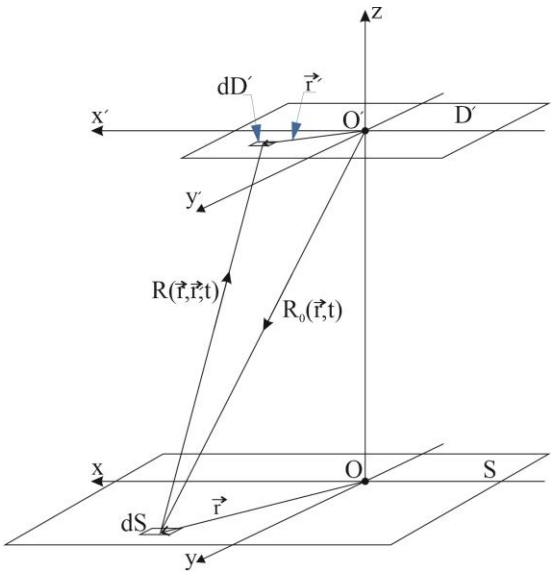

Fig. 4. Geometry of the remote sensing problem

Traditionally, the complex scattering coefficient $\dot{F}(\vec{r},\vec{r}',\vec{\lambda}(\vec{r}))$ is written as a function of the underlying surface coordinates $\vec{r}$. In the task of object injection into the radio image, this should be considered because the object looks different at different viewing angles. At the same time, when the SAR radiation pattern is relatively narrow and oriented normal to the carrier movement direction (side-looking mode) and does not follow a specific area (as is typical in the spotlight mode), the dependence of the complex scattering coefficient on the mutual position of the virtual object and SAR can be neglected.

We assumed that the signal was emitted from the point at which the phase center of the onboard SAR antenna was located (from pt. O', Fig. 4). The electromagnetic field propagates to the underlying surface within the area irradiated by the radiation pattern, and it is reflected by each elementary area (for example, see dS in Fig. 4, the distance to which is $R_0(\vec{r},t)$) and then part of this field is received by the receiving elements (elementary areas dD') of the onboard SAR antenna (distance is given as $R(\vec{r},\vec{r}',t)$). Here, it is assumed that the underlying surface is not mirror-like (e.g., water surface in windless weather) and contains a diffuse component, which is typical for most practical [23, 24] situations that arise in remote sensing.

The signal reflected by the area of the underlying surface irradiated by the radiation pattern of the onboard SAR antenna within the *i*-th range band and received by the elementary antenna area with coordinates $\vec{r}'$, can be written as

$$\dot{s}_{rec}(t,\vec{r}') = \varepsilon\exp(j\varphi)\int_{D_i}\dot{F}(\vec{r},\vec{r}',\vec{\lambda}(\vec{r}))\times \times\dot{G}(\vec{r}-\vec{V}(t-t_0))\dot{A}(t-t_d(t,\vec{r},\vec{r}'))\times \times\exp(j2\pi f_0(t-t_d(t,\vec{r},\vec{r}')))d\vec{r}, \quad (2)$$

where ε is the signal attenuation coefficient, φ is the random initial phase of the signal (evenly distributed in the range of $[0,2\pi]$, $\dot{G}(\vec{r}-\vec{V}(t-t_0))$ is the antenna pattern recalculated to the underlying surface coordinates, and $t_d(t,\vec{r},\vec{r}') = \dfrac{R_0(O',\vec{r},t)+R(\vec{r},\vec{r}',t)}{c}$ is the signal delay time.

For the case in which the SAR antenna focuses the received signals at a precalculated phase center, rather than at each point of the antenna with $\vec{r}'$ coordinates, instead of signal (2), the following should be written:

$$\dot{s}_{rec}(t) = \varepsilon\exp(j\varphi)\int_{D'}\int_{D}\dot{F}(\vec{r},\vec{r}',\vec{\lambda}(\vec{r}))\times \times\dot{G}(\vec{r}-\vec{V}(t-t_0))\dot{A}(t-t_d(t,\vec{r},\vec{r}'))\times \times\exp(j2\pi f_0(t-t_d(t,\vec{r},\vec{r}')))d\vec{r}dr', \quad (2a)$$

where it is taken into account that the SAR antenna is designed so that the delay caused by the signal delay within the antenna aperture (in $\vec{r}'$) is compensated (the signal is focused in the antenna phase center in phase for all points $\vec{r}' \in D'$), otherwise, an additional multiplier must be accounted for the integral $\exp(j\upsilon(\vec{r}'))$, where $\upsilon(\vec{r}')$ is a phase addend that compensates the phase difference of signals received in the antenna phase center and at the antenna point with coordinates $\vec{r}'$.

When an elementary signal (reflected by an elementary area ΔS of the underlying surface with coordinates $\vec{r}$) is received by focusing in the phase center of the aperture D' antenna, we obtain

$$\dot{s}_{rec}(t,\vec{r}) = \varepsilon\exp(j\varphi)\int_{D'}\dot{F}(\vec{r},\vec{r}',\vec{\lambda}(\vec{r}))\times \times\dot{G}(\vec{r}-\vec{V}(t-t_0))\dot{A}(t-t_d(t,\vec{r},\vec{r}'))\times \times\exp(j2\pi f_0(t-t_d(t,\vec{r},\vec{r}')))d\vec{r}'. \quad (2b)$$

ISSN 1814-4225 (print)
ISSN 2663-2012 (online)

In future, when working with signal (2), its notation will clarify which form (2), (2a), or (2b) is meant.

Signal (2) considers that in the process, the mutual positioning in the "phantomization radar–SAR" system changes due to the movement of the SAR carrier. Time t_0 describes the beginning of the interaction between PhR and SAR. Formally, it can be set to zero.

The overall signal model (2) is important for the design of the phantomization system. Some parameters or functions of the signal model (2), such as $\dot{A}(t)$ and $\dot{G}(\vec{r})$, can be estimated in the receiver Rx (Fig. 3) or can be known in advance. The delay time and its change during the satellite movement should be calculated from the actual location of the phantomization radar and the orbit with the satellite's motion laws.

Note that signal (2) is always received in the presence of noise. In our problem, it is sufficient to limit ourselves to additive noise, which is the internal noise $n(t)$ of the receiver. Accordingly, the observation equation can be written as follows:

$$u(t) = \mathrm{Re}\dot{s}_{rec}(t) + n(t) = s_{rec}(t) + n(t). \qquad (3)$$

We will not specify the statistical characteristics of the observation and noise now, because we will return to this issue directly in solving the problem of statistical algorithm synthesis for optimal signal processing in SAR.

6. General Design of the Onboard SAR in Terms of the General Application Model

Previous studies [23, 25-27] have presented block diagrams of onboard SAR, which usually have different details but always contain the key elements of the signal-processing algorithm. Considering that the developing theory should solve the problem of system synthesis, we briefly describe the algorithm synthesis of the radio image formation of an onboard SAR.

In any case, signal processing algorithms in SAR, as justified by the statistical theory of remote sensing radio systems [23] from the standpoint of algorithm synthesis for optimal signal processing, are reduced to matched observation filtering (we are talking about the so-called "classical SAR" [23]). At the level of complex envelopes, the signal processing algorithm is expressed as follows:

$$Y(\vec{r}) = \left| \int_0^T \dot{U}(t)\dot{S}^*_{unit}(t,\vec{r})\,dt \right|, \qquad (4)$$

where $\dot{S}^*_{unit}(t,\vec{r})$ is the unit signal complex envelope (the signal that is used as a predicted signal for a given distance range).

Following (4), a generalized block diagram of SAR in the general model of phantomization radar applications is shown in Fig. 5.

The following notations are used in Fig. 5: A – SAR antenna, AS – antenna switch, Input path – receiver path with high-frequency amplifiers; Tx – SAR transmitter, PD – phase detector unit, RO – reference oscillator, which outputs complex-conjugate signals for phase detectors and synchronizes the transmitter operation, RSG – $\mathrm{Re}(\dot{S}_{unit}(t,\vec{r}))$ and $\mathrm{Im}(\dot{S}_{unit}(t,\vec{r}))$ reference signal generator, RIF – radio image former, which implements signal accumulation (integration in (4)) and calculates the complex radio image modulus, PhR – phantomization

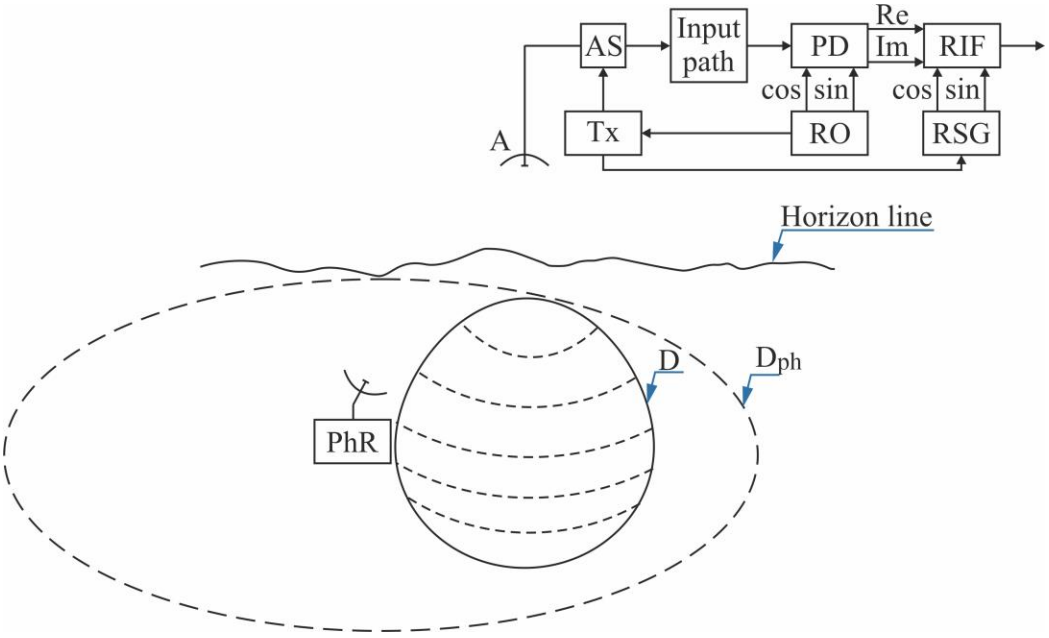

Fig. 5. Generalized block diagram of SAR in phantomization radar application model

radar. Fig. 5 also shows the area D – the area of irradiation of the underlying surface by a synthetic aperture radar (equal range bands are shown) and the area D_{Ph} – the area where the PhR can form a radio image replacement.

When designing a model, it is important that condition $D_{Ph} \geq D$ is satisfied. The condition is achieved by signal generation.

7. Determining the Time of "Interaction" in the "SAR-PhR" System for a Circular Satellite Orbit

Suppose a hypothetical circular orbit with an altitude relative to the Earth's surface (the Earth model is assumed to be an ideal spherical surface).

Fig. 6 shows such an orbit and provides the basic notations necessary for calculating the "interaction" time in the "SAR–PhR" system.

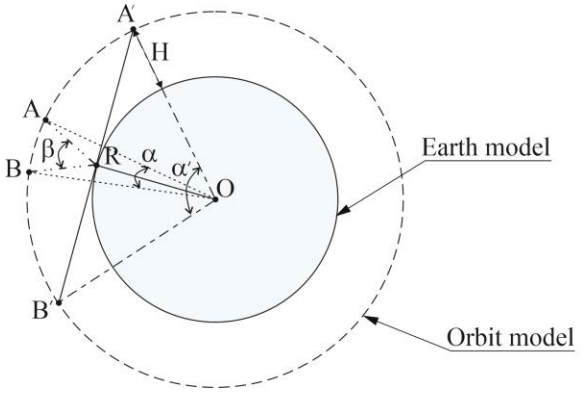

Fig. 6. Geometry for calculating the "interaction" time in the "SAR–PhR" system

The following notations are used in Fig. 6: H is the height [km] of the satellite's orbit relative to the Earth's surface, R is the location of the PhR, O is the Earth's center, OR is the Earth's radius [km], A' and B' are the points of potential beginning and end of the "interaction" of the "SAR–PhR" system, A and B are the points of beginning and end of the "interaction" of the "SAR–PhR" system, $\angle\alpha' = \angle A'OB'$, $\angle\beta$ is the angle in the orbit plane (in Fig. 6, it visually coincides with $\angle ARB$, but in the three-dimensional problem statement it will correspond to $\angle AR'B$, where R' is a perpendicular lowered from pt. X to the orbit projection on the underlying surface (Fig. 7), $\angle\alpha = \angle AOB$, $\angle A'RO = \angle B'RO = 90^\circ$.

The "interaction" time depends on both the mutual position of the "SAR–PhR" system and the satellite's speed, which we denote by V [km/s].

First, let's calculate the potential time t_{pot} of "interaction" – the time that the "SAR–PhR" system may interact, but due to the distances and angles of SAR sensing, this time is impractical to use fully in practice.

Time of potential "interaction" of the "SAR–PhR" system

$$t_{pot} = \frac{\alpha'(OR + H)}{V}. \quad (5)$$

In practice, SAR less often uses the spotlight mode (the pattern beam observes a specific area of the underlying surface in a specific angle range) and more often forms images in the side-looking mode (the pattern is directed at an angle of 90° to the flight line). Let us limit ourselves to the $\angle\beta \leq 90^\circ$ angle (Fig. 6) of the "interaction" of the "SAR–PhR" system, which can be practically achieved by implementing the SAR spotlight mode.

Time of real "interaction"

$$t_{real} = \frac{(OR + H)}{V} \times \times \left(\beta - 2\arcsin\left(\frac{OR}{OR + H}\sin\left(\pi - \frac{\beta}{2}\right)\right)\right). \quad (6)$$

Thus, the obtained equation (6) connects the actual expected time of "interaction" of the SAR-PhR system with the satellite orbit altitude, speed, and the SAR viewing mode ("spotlight" or "side-looking"). When the SAR uses the "side-looking" mode, $\angle\beta = \Delta\theta$, where $\Delta\theta$ is the beamwidth of the SAR radiation pattern (excluding synthetic antenna aperture).

Example. Let SAR works in a spotlight mode and $\angle\beta = 90^\circ$, and let the satellite's altitude be $H = 400$ [km] and flight speed be $V = 7.91$ [km/s]. The Earth's radius is $OR = 6371$ [km]. With these initial parameters, the time of potential "interaction" according to (6) is $t_{real} \approx 98.4$ [s].

In the case of the side-looking mode $\angle\beta = \Delta\theta = 0.6^\circ$ and given that the other parameters from the previous example remain the same, the time of real "interaction" is $t_{real} \approx 0.5$ [s].

Considering that the real interaction time is very short, the PhR system should be designed to interfere with the SAR operation even before the direct SAR–PhR interaction. This means that PhR should be able to be proactive in cases where SAR is operating in the side-looking mode.

8. Equation for the Distance Between SAR and PhR

To calculate the distance between SAR and PhR, we used the geometry shown in Fig. 7, which shows the Earth model, the circular orbit model, the projection of the orbit (trajectory) onto the underlying surface, and the

ISSN 1814-4225 (print)
ISSN 2663-2012 (online)

central view line of the Earth's surface by the satellite from orbit (let's assume that the PhR is located on this line, although this is not essential).

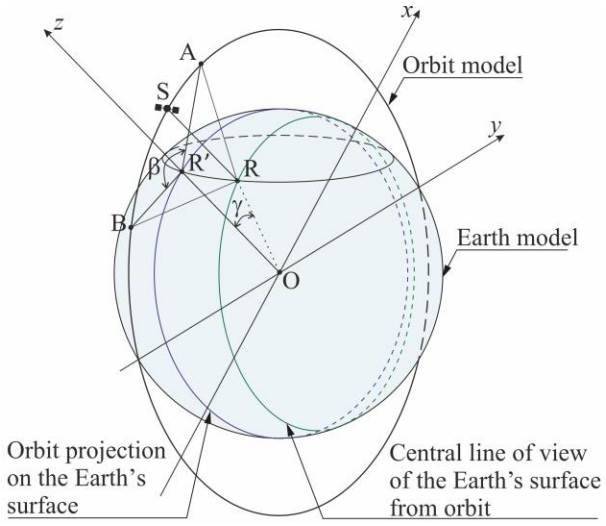

Fig. 7. Geometry for calculating the distance between SAR and PhR

As shown in Fig. 6 in Fig. 7 pt. O is the Earth's center, pt. R is the PhR location, pts. A and B are the beginning and end of the "interaction" in the "SAR-PhR" system, $\angle\beta = \angle AR'B$ is an angle in the plane of the satellite's movement, $\angle\gamma = \angle ROR'$, S is the current position of the SAR satellite, Oxyz is a three-dimensional Cartesian coordinate system associated with the Earth's center, the Oz axis of which goes through pt. R′ (a perpendicular lowered from pt. R to the projection of the satellite's orbit on the underlying surface, $OR = OR'$).

The general equation for the distance between the orbital elements and the PhR location, whose location is denoted by the X coordinates, is as follows:

$$\Delta Q = \sqrt{\left(\sqrt{(OR'+H)^2 - z^2} - X_R\right)^2 + Y_R^2 + (z - Z_R)^2}. \quad (7)$$

The resulting expression (7) is general and describes the distance between the PhR and the SAR, which is located anywhere in its orbit. The orbit segment between pt. A and pt. B the parameter z should be properly constrained.

9. Expected Packet Length and Number of Radio Pulses Within the Onboard SAR Signal Packet

In (1), a coherent packet of radio pulses is used in the onboard SAR sensing signal (in particular, in the form of an M-sequence with monochrome content or, in more complex cases, with linear frequency modulation (LFM)). The complex envelope of a radio pulse packet can be written as follows:

$$\dot{A}(t) = A_0 \sum_{i=0}^{N-1} I_i S(t - iT_r, \tau) \exp\left(j\pi\alpha(t - iT_r)^2\right), \quad (8)$$

where A_0 is the amplitude of radio pulses in a packet, N is the number of radio pulses in a packet, I_n is a sign function that, when using LFM pulses with phase-shift keying in a packet, can define a phase change within a pulse to the opposite by using "1" or "-1", T_r is the period of radio pulses in the packet, $\alpha = \frac{\Delta F}{\tau}$, ΔF is the frequency deviation of the LFM pulse, $S(t - iT_r, \tau)$ is a cut-off function that describes an envelope of one radio pulse in the packet, which is usually a flat video pulse, with a length of τ and a pulse repetition period of $T_r > \tau$, i.e.

$$S(t - iT_r, \tau) = \begin{cases} 1 & 0 \le (t - iT_r) \le \tau; \\ 0 & (t - iT_r) < 0, \ (t - iT_r) > \tau, \end{cases}$$

or describes, for example, the envelope of an M-sequence.

To solve the problem of estimating the sensing signal parameters of the onboard SAR, it is necessary to understand the length of the radio pulse packet and the number of N pulses in the packet. It is necessary to state the problem of optimal PhR receiver synthesis.

Fig. 8 shows the geometry of the problem for deriving the expression for the maximum length of the sensing signal packet and the minimum repetition period of the onboard SAR sensing signal packets. The angles q_{min} and q_{max} determine the minimum and maximum irradiation angle of the underlying surface and correspond to the ranges R_{min} and R_{max}.

The maximum length of the radio pulse packet (length of the M-sequence) is calculated by assuming that the transceiver should be closed (do not emit radio pulses) when the pulses reflected by the underlying surface start receiving. Therefore, the time required for a radio pulse to pass a double minimum distance R_{min} determines the maximum length of a radio pulse or a packet of radio pulses as follows:

$$t_b = \frac{2H}{c \cdot \cos(q_{min})}, \quad (9)$$

where c is the speed of light.

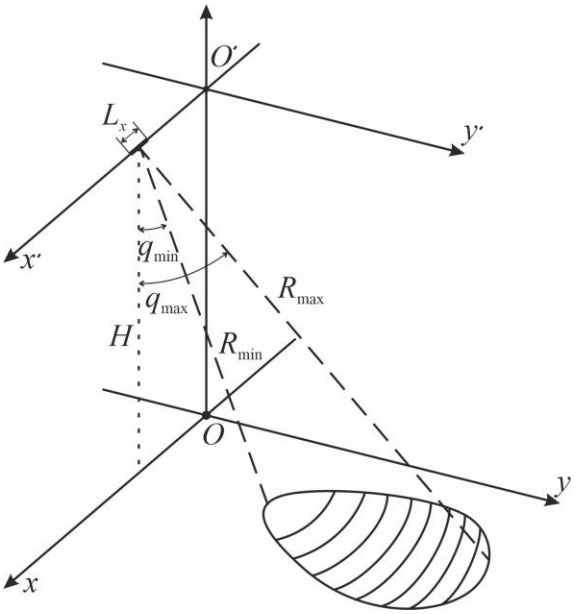

Fig. 8. Problem geometry for determining the equation for the maximum length of the sensing signal packet and the minimum repetition period of the onboard SAR signal packets

The repetition period of radio pulse packets is determined by the time required for the last pulse in the packet to pass twice the maximum distance (length t_b), so let's find the minimum repetition time (period) of the pulse packets as follows:

$$T_b = \frac{2H\left(\cos(q_{min}) + \cos(q_{max})\right)}{c \cdot \cos(q_{max})\cos(q_{min})}. \qquad (10)$$

The pulse inverse duty cycle in a packet is determined by the capability of the radio components. The possible value of the inverse duty cycle for these problems is $Q = 4$. The number of pulses in a packet is given by

$$N = \left\lfloor \frac{2H}{T_r \cdot c \cdot \cos(q_{min})} - \frac{\tau}{T_r} + 1 \right\rfloor, \qquad (11)$$

where $\lfloor \cdot \rfloor$ – is the operator brackets rounding down.

In addition, for this problem, it is advisable to discuss the inverse duty cycle of the probing signal packets, which is defined as follows:

$$Q_b = \frac{T_b}{t_b} = \frac{R_{max} + R_{min}}{R_{min}} = \frac{R_{max}}{R_{min}} + 1 = \\ = \frac{\cos(q_{min})}{\cos(q_{max})} + 1. \qquad (12)$$

Fig. 9 shows the radio pulse packet envelope containing the above notations.

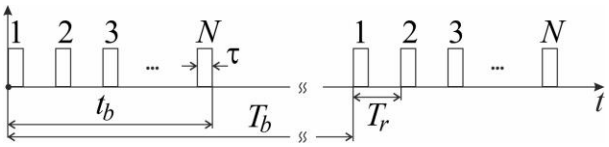

Fig. 9. An envelope containing two packets of radio pulses with the introduced notations

10. Relation Between the Spaceborne SAR Sensing Signal and the Synthetic Antenna Pattern

The sensing signal (1), considering the previous statements, also affected the shape of the synthesized SAR radiation pattern. Let us consider this impact for the following reasons.

To form a single radio image cross-section along the line of sight of the antenna pattern, a packet of radio pulses will be used. Typically, previous studies [22, 25-27] have discussed the use of a single sensing pulse to form a cross-section of the radio image along the line of sight of the antenna pattern. In practice, a packet of radio pulses is used to increase the spatial resolution over a range and to increase the energy.

If not a single cross-section of the radio image is created but a radio image frame, it is advisable to represent the complex envelope (1), with the above notations, as a packet of radio pulses packets (for example, taking into account the pulses content with LFM signals):

$$\dot{A}(t) = A_0 \Pi\left(\frac{t}{T_{bb}}\right)\left(\sum_k S_\delta(t - kT_b) \otimes \Pi\left(\frac{t}{t_b}\right)\right) \times \\ \times \left(\sum_n I_n S_\delta(t - nT_r) \otimes \left[\Pi\left(\frac{t}{\tau}\right)\exp\left(j\pi\alpha t^2\right)\right]\right), \qquad (13)$$

where $\Pi\left(\frac{t}{T_{bb}}\right)$ is the envelope of a pulse packet (cutoff function), which describes the radiation pattern of a real SAR antenna but can sometimes be approximated by a uniform function of the length T_{bb} of the pulse packet, $S_\delta(t)$ is the Dirac delta function, $\Pi\left(\frac{t}{t_b}\right)$ is the envelope of a single radio pulse packet, which can be described by a uniform function of length t_b, $\Pi\left(\frac{t}{\tau}\right)$ is the envelope of a radio pulse, I_n is a sign function that, when using LFM pulses with phase-shift keying, can define a

ISSN 1814-4225 (print)
ISSN 2663-2012 (online)

phase change within a pulse to the opposite by using "1" or "-1", $\otimes$ is a convolution operator, t is a time variable.

The length of the packet of radio pulse packets is defined as follows:

$$T_{bb} = (m-1)T_b + t_b, \quad (14)$$

where m is the number of pulse packets in the packet.

Substituting (13) into (1) gives the expected form of the emitted signal (1), which becomes the basis for the trajectory received signal:

$$s(t) = A_0 \times \times \mathrm{Re}\left\{\Pi\left(\frac{t}{T_{bb}}\right)\left(\sum_k S_\delta(t-kT_b)\otimes\Pi\left(\frac{t}{t_b}\right)\right)\right\}\times \times \mathrm{Re}\left\{\sum_n I_n S_\delta(t-nT_r)\otimes\left[\Pi\left(\frac{t}{\tau}\right)\exp\left(j\pi\alpha t^2\right)\right]\right\} \times \mathrm{Re}\left\{\exp\left(j2\pi f_0 t\right)\right\}. \quad (15)$$

The obtained equation plays an important role in the optimal system synthesis for estimating the parameters of the onboard SAR sensing signal. This is because the complicated problem of estimating the waveform (1) (belongs to the functional analysis) is replaced by the problem of estimating the parameters of a functionally determined signal (14) without loss of accuracy.

According to the statistical theory of radio engineering systems, we can expect that the optimal signal processing algorithm (to be performed in future stages of work) will include both optimal intra-pulse and intra-packet and inter-packet signal processing. The above impacts the synthesized antenna pattern.

It is known [22] that the SAR radiation pattern can be synthesized from two different approaches:

− in-phase accumulation of reflected signals on the SAR flight path is analogous to the formation of a large antenna aperture in time in space (sometimes also called a phantom antenna array, i.e., one that does not exist at the same time in space);

− processing of the spatial LFM signal, which is a trajectory signal formed from the optimal responses of the reflected signal packets.

Both approaches yielded identical results: synthesized SAR pattern compression.

Let's examine how the packet signal form affects the in-phase accumulation of reflected signals on the SAR flight path. It should be noted that radio pulse packets are received in space in a manner that forms a sparse aperture. From antenna array theory, it is known that a sparse antenna array forms a multi-lobe radiation pattern, which is, therefore, followed by ambiguity in radio image formation in angular coordinates.

It is known [22] that the size of the synthesized aperture X along the flight line is defined by the linear resolution of the underlying surface along the flight line:

$$X \approx \frac{\lambda}{L}\frac{H}{\cos(q_{av})}, \quad (16)$$

where L is the size of the aperture of the real (fuselage) onboard radar antenna, λ is the wavelength of the onboard radar,

$$q_{av} = \frac{q_{max}+q_{min}}{2}, \quad (17)$$

is the average value of the underlying surface's viewing angle in the angular plane.

This value X is related to the length of the packet of pulse packets as follows

$$X = VT_{bb}, \quad (18)$$

or

$$\frac{\lambda}{L}\frac{H}{\cos(q_{av})} = V\left((m-1)T_b + t_b\right),$$

where V is the satellite speed.

Hence, we find the relationship between the pulse packet number in the packet m and the signal parameters, antenna, and imaging geometry as follows:

$$m = \frac{\lambda}{L}\frac{H}{VT_b\cos(q_{av})} - \frac{t_b}{T_b} + 1, \quad (19)$$

or, taking into account (9), (10), and (17), the number of packets of radio pulse packets is defined as follows:

$$m = \frac{1}{2}\frac{\lambda}{L}\times \times \frac{c\cdot\cos(q_{max})\cos(q_{min})}{V\left(\cos(q_{min})+\cos(q_{max})\right)\cos\left(\frac{q_{max}+q_{min}}{2}\right)} - \frac{\cos(q_{max})}{\cos(q_{min})+\cos(q_{max})} + 1.$$

Example. Let's find the values calculated by expressions (16), (19), and (14) for the flight conditions considered above: $H = 400$ [km], $L = 13.3$ [m], $q_{min} = 20^\circ$, $q_{max} = 50^\circ$, $V = 7910$ [m/s]. Using (16), (19) i (14) we'll get $X \approx 1101.5$ [m], $m \approx 20$, $T_{bb} \approx 135.6$ [ms].

Note that equations (16)-(19) are approximate because they ignore the curvature of the satellite's flight path around the irradiated area of the underlying surface. Let us consider the impact of trajectory curvature and its differences from straight flight, which is usually chosen as the basis for calculations of synthetic aperture systems. To calculate the distance difference between an SAR moving along a curvilinear trajectory in the orbit between pt. A and pt. B and a hypothetical straight line AB (Fig. 7) of length X we use (7), as well as the distance change equation from pt. R to the line AB (Fig. 7) in the following form:

$$\Delta Q_{AB} = \sqrt{(x - X_R)^2 + Y_R^2 + (z - Z_R)^2}, \quad (20)$$

where the coordinate x varies within $[-X/2, X/2]$, and $z = OC = (OR' + H)\cos\left(\arcsin\left(X/2(OR' + H)\right)\right)$.

We can write (20) in the final view as follows:

$$\Delta Q_{AB} = \sqrt{\begin{array}{c}(x - X_R)^2 + Y_R^2 + \\ +\left((OR' + H)\times \right. \\ \left. \times\cos\left(\arcsin\left(\dfrac{X}{2(OR' + H)}\right)\right) - Z_R\right)^2\end{array}}. \quad (21)$$

The distance difference is then calculated as

$$\Delta R = \Delta Q - \Delta Q_{AB} = \sqrt{\begin{array}{c}(x - X_R)^2 + Y_R^2 + \\ +\left((OR' + H)\times \right. \\ \left. \times\cos\left(\arcsin\left(\dfrac{X}{2(OR' + H)}\right)\right) - Z_R\right)^2\end{array}}, \quad (22)$$

where ΔQ is given by (7).

Example. Satellite flight height $H = 400$ [km]. Earth's radius $OR' = 6371$ [km]. The SAR implements the view within the SAR movement limited by the angle $\alpha = 2\arcsin\left(\dfrac{X}{2(OR' + H)}\right)$ along the line AB, with a length of $X \approx 1101.5$ [m] see (16) and the previous example). The coordinates of the PhR location are assumed to be $(0, 100, OR')$.

Fig. 10 shows the distances ΔQ and ΔQ_{AB}, calculated according to (7) and (21), which vary within the angle $\alpha = 2\arcsin\left(\dfrac{X}{2(OR' + H)}\right)$. Fig. 11 shows the difference between these distances $\Delta R = \Delta Q - \Delta Q_{AB}$ (see (22)) in [cm].

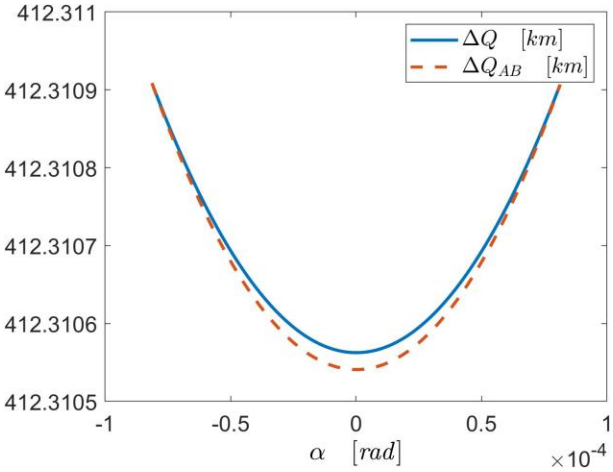

Fig. 10. The distances ΔQ and ΔQ_{AB} calculated according to (7) and (21), which varied within the angle $\alpha = 2\arcsin\left(\dfrac{X}{2(OR' + H)}\right)$

The minimum curve in Fig. 10 corresponds to the minimum distance between the SAR and the PhR. At the same time, the distance between the SAR and the PhR up to this point initially decreases, and then increases, because the point is located along the normal in the SAR direction to the line (see Fig. 6), which is traced to the Earth model at the PhR location (see p. R in Fig. 6).

It is expected that at the observation edges (see Fig. 11), the distance difference will be zero because the coordinates of the simplified and real trajectories at these points are the same.

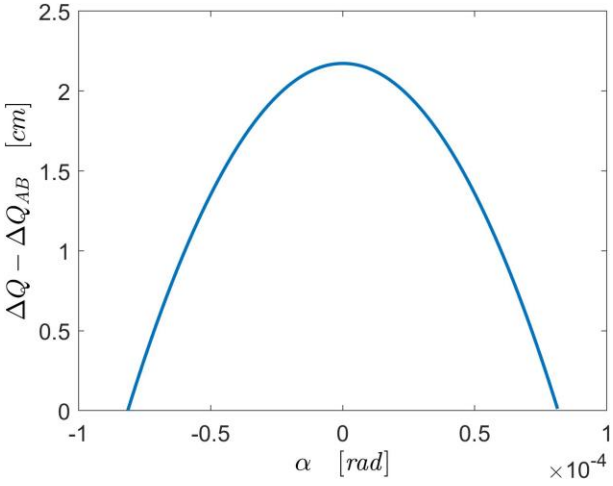

Fig. 11. Distance difference $\Delta R/\lambda = \Delta Q - \Delta Q_{AB}/\lambda$ (see (22)) in [cm]

Fig. 12 shows the distance difference in wavelengths $\dfrac{\Delta R}{\lambda} = \dfrac{\Delta Q - \Delta Q_{AB}}{\lambda}$ for the wavelength $\lambda = 3$ [cm].

ISSN 1814-4225 (print)
ISSN 2663-2012 (online)

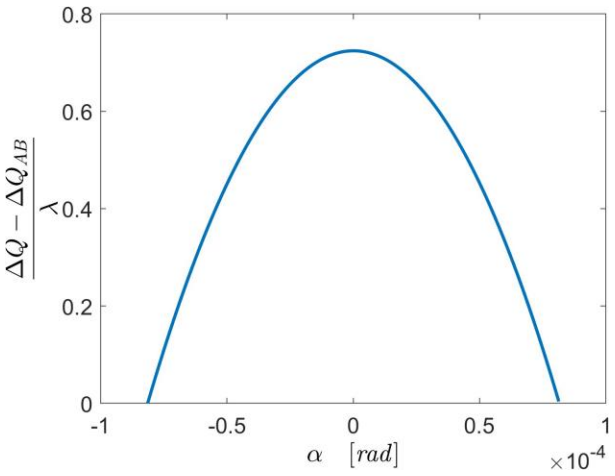

Fig. 12. Distance difference in wavelengths $\Delta R/\lambda = \Delta Q - \Delta Q_{AB}/\lambda$ for the wavelength $\lambda = 3$ [cm]

The extremum in Figs. 11 and 12 corresponds to the point of maximum discrepancy in the distance in the "SAR-PhR" system calculated using the two assumptions that were made when deriving formulas (7) and (21).

The analysis in Fig. 12 shows that the distance difference obtained using the simplified (linear) trajectory of the onboard SAR in the above calculations did not exceed 0.75 wavelengths toward the synthetic aperture center. Therefore, the previous calculations allow us to correctly estimate the values.

11. Discussion

Overall, the idea is that "if the radio image can be distorted, then it can also be edited (phantoms can be added) with the help of information 'injection' signals into the radio image" and the hypotheses are confirmed by preliminary calculations. It has been shown (Fig. 3) that the radar should fundamentally contain the following units: a receiver that evaluates the form, parameters, and characteristics of the SAR sensing signal, a memory unit that accumulates this information based on different SAR observation modes, and a unit of object characteristics that need to be injected into the phantomization signal emitted by the radar.

Of course, developing this theory is quite challenging because, in addition to the above partial tasks, it is important to ensure the synchronized imposition of the injection signal so that the SAR recognizes it "as a naturally formed object on the underlying surface". Such synchronization eliminates the need to model the signal with the underlying surface, simplifying generating a radio image replacement signal. It is also desirable to match the injection signal with the signal reflected by the underlying surface in power. Otherwise, this may become information characteristic in the future that will allow decision-making regarding intervention in the SAR imaging process.

The obtained equations for aligning the problem geometry with the signal parameters allow us to obtain preliminary information (see (9)-(12), (14), (19)) for the future solution of the receiver optimization task by statistical synthesis methods (Hypothesis 5 is proved). At the same time, the preliminary estimates of various parameters of the signals in the packet allow us to set the task of algorithm synthesis for estimating not the waveform in the receiver design but to move on to estimating individual parameters and characteristics of the sensing signal—pulse duration, pulse sequence in the packet, number of pulses in the packet, number of pulse packets involved in the radio image pixel formation process, carrier frequency or type of modulation of each pulse, etc. Even the transition to this number of parameters and estimation characteristics simplifies the problem of optimal receiver synthesis, which can be much more difficult through the synthesis of an optimal waveform estimator. In the latter case, a much larger amount of a priori data is required in the form of an admissible function class for identifying the optimal solution. The a priori data on the possible values of the sensing signal parameters are functionally defined in this paper along with the possible geometries of the underlying surface sensing.

As shown, the underlying surface observation geometry limits all parameters and signal form. The satellite flight height, orbit shape, viewing angle, and observation mode. In particular, Figs. 10-12 also show the validity of Hypothesis 4 regarding the need to consider information about the relative movements of the SAR and the PhR. The distance change in this system affects the signal's information characteristics.

The main information about the underlying surface and the objects on it is contained in the complex scattering coefficient. This coefficient (actually a complex function of angular coordinates, object geometry, and object materials) should be calculated in advance for different types of objects to be injected into the image in the future. The process of injecting this coefficient into the radio image replacement signal requires changing its parameters during the addition process because the visibility of the object from the SAR changes during mutual movement. In addition, when injecting objects that move relative to the underlying surface, this should also be considered by both changing the Doppler frequency and changing the visibility portrait from the SAR.

Note that Hypotheses 1-3 will be proved in the further development of radio image phantomization theory.

12. Conclusions

Let's summarize the results of the research.

The concept of PhR design. PhR should include the following:

– a receiver at which the form, parameters, and characteristics of the SAR signal must be estimated;

– a model bank of SAR signals;

– a model bank of objects to be injected into the PhR signal;

– transmitter that generates a signal with information about the object to be added to the radio image at the SAR output.

The generalized block diagram allows us to obtain all the necessary data for the sensing signal and to inject a signal with objects absent in a specified area within a certain period synchronously with the signal reflected by the underlying surface.

The receiver unit should be designed using the optimal statistical synthesis methods of signal-processing algorithms to estimate the parameters defined in the article:

– pulse duration τ;

– pulse-sequence period in the packet T_r;

– number of pulses in a packet N;

– packet repetition period T_b;

– number of packets required to form one pixel of the radio image m;

– packet length of the radio pulse packets T_{bb};

– center frequency of the pulse f_0;

– pulse modulation type in the packet.

Defining these parameters allows us to solve an optimization problem in receiver synthesis, assuming that the signal is described by a functionally deterministic model with uncertain parameters. This approach significantly simplifies the synthesis problem related to the optimal waveform estimation.

The signal and object model banks to be injected into the radio image can be created using any known data accumulation and storage systems. The requirements of these systems are defined by the write and read speeds and hardware reliability.

The signal transmitter can be designed using optimal synthesis methods or engineering experience. Typically, the transmitter circuit is simpler than the receiver circuit because of the principles of optimal signal processing. When emitting the injection signal, it is important to synchronize it by distance (distance strips) with the signals reflected by the underlying surface.

PhR application geometry. The interaction geometry in the "SAR-PhR" system is discussed. The analysis of the geometry allowed us to determine the equation for the distance ΔQ between SAR and PhR, as well as to estimate the parameters related to the distance (signal delay time and parameters of the sensing signals).

The concept and the corresponding equation for the potential interaction time t_{pot} in the "SAR-PhR" system and the real time t_{real} of such an interaction are defined.

The SAR radiated and reflected by the underlying surface signals are determined. The place of the information component (the complex scattering coefficient) in the signal is shown, which is important for the formation of an accurate model of the emitted signal.

The obtained equations contain information about the geometric parameters (viewing angles, height, distance, orbit, etc.) of the SAR application and its speed.

Future research directions. As noted earlier, this paper outlines the fundamentals of radio image phantomnation theory for remote sensing satellites. Further scientific research on this topic includes the development of novel models of spatiotemporal trajectory radio signals with information about "phantoms" (such models will take into account the scattering characteristics of areas), the development of new methods for adding fake signals to trajectory signals, and the analysis of criteria and factors limiting the application of such a phantomization theory.

Contribution of authors: conceptualization – **Volodymyr Pavlikov**, **Simeon Zhyla**; ideas, hypotheses, and problems statements – **Volodymyr Pavlikov**, **Simeon Zhyla**; SAR signals and transformation calculations – **Eduard Tserne**, **Pavlo Malashta**, **Hlib Cherepnin**; design of onboard SAR development – **Olexandr Shmatko**, **Oleksii Odokiienko**; time of interaction in "SAR–PhR" system calculations – **Volodymyr Pavlikov**; "SAR–PhR" distances equations determination – **Simeon Zhyla**, **Hlib Cherepnin**, **Eduard Tserne**; calculations on packet length and radio pulses number within the onboard SAR signal packet – **Olexandr Shmatko**, **Pavlo Pozdniakov**; calculations on relations between the spaceborne SAR sensing signal and the synthetic antenna pattern – **Volodymyr Pavlikov**, **Oleksii Odokiienko**; writing original draft – **Volodymyr Pavlikov**, **Simeon Zhyla**, **Denys Kolesnikov**; review and editing – **Volodymyr Pavlikov**, **Pavlo Pozdniakov**, **Denys Kolesnikov**.

Conflict of Interest

The authors declare that they have no conflict of interest in relation to this research, whether financial, personal, author ship or otherwise, that could affect the research and its results presented in this paper.

Financing

This research was supported by the Ministry of Education and Science of Ukraine. The state registration number of the project "Radio engineering systems theory of phantom radio imaging for aerospace-based radars" is 0124U001015.

Project information

Project 0124U001015 aims to develop a new theory of radio image phantomization (adding phantom parts to

ISSN 1814-4225 (print)
ISSN 2663-2012 (online)

the image), which are formed by remote sensing radars from aerospace carriers, and to develop recommendations for the construction of appropriate radio systems.

In general, the project's objectives include: to develop the fundamentals of the radio engineering systems theory, which replaces/adds to the radio images for aerospace remote sensing systems according to predefined scenarios; creating new components of the theory of estimating the parameters of signals emitted by aerospace remote sensing systems; creating new mathematical models of spatiotemporal trajectory radio signals containing information about the "phantoms" on the areas of the underlying surface; developing new methods of adding "injection" signals to the trajectory signals formed by radiovision systems; adjusting signal mathematical models to reflect the atmosphere state and the polarization processing features of sensing signals; and giving recommendations on the application of the new theory for the engineering implementation of radars, analysis of theory application limitations.

Data Availability

The manuscript contains no associated data.

Use of Artificial Intelligence

The authors confirm that they did not use artificial intelligence methods in their work.

All the authors have read and agreed to the publication of the final version of this manuscript.

References

1. Goward, S. N., Bauer, M. E., Biehl, L. L., Hall, F. G., Hoffer, R. M., Richards, J. A., Rocchio, L. E. P., Salomonson, V. V., & Williams, D. L. David A. Landgrebe: Evolution of Digital Remote Sensing and Landsat. *IEEE Journal of Selected Topics in Applied Earth Observations and Remote Sensing*, 2022, vol. 15, pp. 4835-4860. DOI: 10.1109/JSTARS.2022.3176804.

2. Sumantyo, J. T. S, Chua, M. Y., Santosa, C. E., Panggabean, G. F., Watanabe, T., Setiadi, B., Sumantyo, F. D. S., Tsushima, K., Sasmita, K., Mardiyanto, A., Supartono, E., Rahardjo, E. T., Wibisono, G., Marfai, M. A., Jatmiko, R. H., Sudaryatno, Purwanto, T. H., Widartono, B. S., Kamal, M., Perissin, D., Gao, S., & Ito, K. Airborne Circularly Polarized Synthetic Aperture Radar. *IEEE Journal of Selected Topics in Applied Earth Observations and Remote Sensing*, 2021, vol. 14, pp. 1676-1692. DOI: 10.1109/JSTARS.2020.3045032.

3. Jin, Y., Chen, J., Xia, X. G., Liang, B., Xiong, Y., Liang, Z., & Xing, M. Ultrahigh-Resolution Autofocusing for Squint Airborne SAR Based on Cascaded MD-PGA. *IEEE Geoscience and Remote Sensing Letters*, 2022, vol. 19, article no. 4017305. DOI: 10.1109/LGRS.2021.3105254.

4. Pavlikov, V., Volosyuk, V., Zhyla, S., Van, H. N., & Van, K. N. A new method of multi-frequency active aperture synthesis for imaging of SAR blind zone under aerospace vehicle. *Proceedings of the 2017 14th International Conference The Experience of Designing and Application of CAD Systems in Microelectronics (CADSM)*, Lviv, Ukraine, IEEE, 2017, pp. 118-120. DOI: 10.1109/CADSM.2017.7916099.

5. Wang, D., Gao, Q., Liu, Z., Ding, Y., Huang, T., & Gao, L. Evaluation of Vehicle Camouflage Effectiveness under a Complex Background Based on the Time-Limited Search Model. *IEEE Journal of Selected Topics in Applied Earth Observations and Remote Sensing*, 2022, vol. 15, pp. 6133-6143. DOI: 10.1109/JSTARS.2022.3192351.

6. Zhao, J., Zhou, B., Wang, G., & Liu, J. Camouflage Target Recognition Based on Dimension Reduction Analysis of Hyperspectral Image Regions. *IEEE Journal of Selected Topics in Applied Earth Observations and Remote Sensing*, 2022, vol. 15, pp. 6133-6143. DOI: 10.1109/JSTARS.2022.3192351.

7. Kavipriya, P., Jegan, G., Venkat, E., & Ranganadh, D. N. Design of IOT Based Multifunctional Camouflage Military Robot. *Proceedings of the 2021 International Conference on Artificial Intelligence and Smart Systems (ICAIS)*, Coimbatore, India, IEEE, 2021, pp. 1431-1435. DOI: 10.1109/ICAIS50930.2021.9395991.

8. Shimoni, M., Haelterman, R., & Perneel, C. Hyperspectral Imaging for Military and Security Applications: Combining Myriad Processing and Sensing Techniques. *IEEE Geoscience and Remote Sensing Magazine*, 2019, vol. 7, no. 2, pp. 101-117. DOI: 10.1109/MGRS.2019.2902525.

9. Luo, Y., Guo, L., Zuo, Y., & Liu, W. Time-Domain Scattering Characteristics and Jamming Effectiveness in Corner Reflectors. *IEEE Access*, 2021, vol. 9, pp. 15696-15707. DOI: 10.1109/ACCESS.2021.3053116.

10. Praja, M., & Pamungkas, W. Linear Polarization on Radar Cross Section Measurement for Tank Miniature. *INFOTEL*, 2022, vol. 14, no. 4, pp. 263-268. DOI: 10.20895/infotel.v14i4.782.

11. Qingyang, S., Ting, S., Kai-Bor, Y., & Wenxian, Y. Fast Target Deception Jamming Method against Spaceborne Synthetic Aperture Radar Based on Equivalent Bistatic Scattered Fields. *The Journal of Engineering*, 2019, pp. 7385-7389. DOI: 10.1049/joe.2019.0507.

12. Liu, Y. X., Zhang, Q., Xiong, S. C., Ni, J. C., Wang, D., & Wang, H.-B. An ISAR Shape Deception Jamming Method Based on Template Multiplication and Time Delay. *Remote Sensing*, 2023, vol. 15, no. 11, article no. 2762. DOI: 10.3390/rs15112762.

13. Sukharevsky, O., Nechitaylo, S., & Vasilets, V. Using Corner Reflectors to Increase Backscattering of Radar Targets. *Proceedings of the 2020 IEEE Ukrainian Microwave Week (UkrMW)*, Kharkiv, Ukraine, IEEE, 2020, pp. 207-212. DOI: 10.1109/UkrMW49653.2020.9252740.

14. Watanabe, T. Image-Based Radar Cross Section Synthesis for a Cluster of Multiple Static Targets. *IEEE Transactions on Instrumentation and Measurement*, 2023, vol. 72, article no. 8001413. DOI: 10.1109/TIM.2023.3246489.

15. Burlaka, O. *Strange Electromagnetic Interference Was Detected over Crimea*. Available at: https://universemagazine.com/en/strange-electromagnetic-interference-was-detected-over-crimea/ (accessed 14.08.2024).

16. Fevralev, D. V. Ponomarenko, N. N. Lukin, V. V., Mäkitalo, M., & Foi, A. Efficiency Analysis of Color Image Filtering. *EURASIP Journal on Advances in Signal Processing*, 2011, article no. 41. DOI: 10.1186/1687-6180-2011-41.

17. Mäkitalo, M., Foi, A., Fevralev, D., & Lukin, V. Denoising of Single-Look SAR Images Based on Variance Stabilization and Nonlocal Filters. *Proceedings of the 2010 International Conference on Mathematical Methods in Electromagnetic Theory*, Kyiv, Ukraine, IEEE, 2010, pp. 1-4. DOI: 10.1109/MMET.2010.5611418.

18. Zhyla, S., Volosyuk, V., Pavlikov, V., Ruzhentsev, N., Tserne, E., Popov, A., Shmatko, O., Havrylenko, O., Kuzmenko, N., Dergachov, K., Averyanova, Y., Sushchenko, O., Zaliskyi, M., Solomentsev, O., Ostroumov, I., Kuznetsov, B., & Nikitina, T. Statistical Synthesis of Aerospace Radars Structure with Optimal Spatio-Temporal Signal Processing, Extended Observation Area and High Spatial Resolution. *Radioelectronic and Computer Systems*, 2022, no. 1, p. 178-194. DOI: 10.32620/reks.2022.1.14.

19. Volosyuk, V. K., Pavlikov, V. V., Zhyla, S. S., & Van, N. H. Phenomenological Description of the Electromagnetic Field and Coherent Images in Radio Engineering and Optical Systems. *Proceedings of the 2018 IEEE 17th International Conference on Mathematical Methods in Electromagnetic Theory (MMET)*, Kyiv, Ukraine, IEEE, 2018, pp. 302-305. DOI: 10.1109/MMET.2018.8460321.

20. Pavlikov, V. V., Volosyuk, V. K., Zhyla, S. S., & Van, N. H. Active Aperture Synthesis Radar for High Spatial Resolution Imaging. Proceedings of the 9th International Conference on Ultrawideband and Ultrashort Impulse Signals (UWBUSIS), Odessa, Ukraine, IEEE, 2018, pp. 252-255. DOI: 10.1109/UWBUSIS.2018.8520021.

21. Rahmanizadeh, A., & Amini, J. An Integrated Method for Simulation of Synthetic Aperture Radar (SAR) Raw Data in Moving Target Detection. *Remote Sensing*, 2017, vol. 9, no. 10, article no. 1009. DOI: 10.3390/rs9101009.

22. Volosyuk, V. K., & Kravchenko, V. F. *Statisticheskaya teoriya radiotekhnicheskikh sistem distantsionnogo zondirovaniya i radiolokatsii* [Statistical theory of radio-technical systems of remote sensing and radiolocation]. Moscow, Fiziko-matematicheskaya literatura Publ., 2008. 704 p.

23. Kabakchiev, C., Garvanov, I., Behar, V., Kabakchiev, A., & Kabakcueva, D. Forward Scatter Radar Detection and Estimation of Marine Targets. *Proceedings of the 2012 13th International Radar Symposium*, Warsaw, Poland, IEEE, 2012, pp. 533-538. DOI: 10.1109/IRS.2012.6233380.

24. Volosyuk, V., Zhyla, S., & Kolesnikov, D. Phenomenological Description of Coherent Radar Images Based on the Concepts of the Measure of Set and Stochastic Integral. *Telecommunications and Radio Engineering*, 2019, vol. 78, iss. 1, pp. 19-30. DOI: 10.1615/TelecomRadEng.v78.i1.30.

25. Richards, M. A. *Fundamentals of Radar Signal Processing*. 2nd ed. McGraw-Hill, 2014. 656 p.

26. Cutrona, L. J., & Hall, G. O. A Comparison of Techniques for Achieving Fine Azimuth Resolution. *IRE Transactions on Military Electronics*, 1962, vol MIL-6, pp. 119-121.

27. Rahman, H. *Fundamental Principles of Radar*. CRC Press, 2019. 340 p.

Received 17.07.2023, Accepted 18.11.2024

ОСНОВИ ТЕОРІЇ СИНТЕЗУ РАДАРІВ ФОРМУВАННЯ ФАНТОМНИХ ОБ'ЄКТІВ НА РАДІОЗОБРАЖЕННЯХ РСА

В. В. Павліков, С. С. Жила, П. В. Поздняков, Д. В. Колесніков, Г. С. Черепнін, О. О. Шматко, О. В. Одокієнко, П. П. Малашта, Е. О. Церне

Предметом статті є створення основ теорії формування хибних елементів на зображеннях систем аерокосмічного радіобачення. Даний процес передбачає внесення у просторово-часові траєкторні сигнали відсутніх на опроміненій з аерокосмічного носія підстильній поверхні інформаційних ознак об'єктів. **Мета дослідження** полягає у визначенні загальної концепції побудови та застосування радарів фантомізації (РФ) радіозображень. **Завдання**, на вирішення яких спрямовано дослідження: виконати опис загальної концепції побудови та застосування РФ; сформувати гіпотези, які лежать у основі теорії та окреслити коло питань, які підлягають вирішенню; визначити загальну структуру РФ; розробити математичні моделі законів зміни дальності в системі «формувач фантомного зображення – радіосистема дистанційного зондування»; визначити обмеження на розміри ділянки, на якій можна забезпечити фантомне заміщення реальних радіозображень відповідно до режиму огляду підстильної поверхні з супутника. Вирішення поставлених завдань ґрунтуються на **методах** теорії синтезу систем дистанційного зондування, методах радіофізики, методах формування когерентних зображень, функціонального аналізу, синтезу та оброблення просторово-часових сигналів. Отримані наступні **результати**: 1) визначено структуру РФ, яка включає приймач, банк моделей сигналів РСА, банк моделей об'єктів, які необхідно ін'єктувати у сигнал РФ та передавач; 2) визначено параметри прийнятого зондувального сигналу РСА, які необхідно оцінювати у приймачі PhR; 3) розглянуто геометрію взаємодії у системі «РСА-РФ», що дозволило визначити вираз для оцінки дальності між РСА до РФ, а також оцінити

ISSN 1814-4225 (print)
ISSN 2663-2012 (online)

пов'язані з дальністю параметри, такі як час затримки сигналу та характеристики зондувальних сигналів. **Висновки**. Стаття описує широке коло первинних питань, які виникають при формуванні теорії фантомізації радіозображень. Отримані результати є підґрунтям для наступних досліджень, які доцільно спрямувати на розроблення математичних моделей орбіт аерокосмічних систем дистанційного зондування, просторово-часових сигналів випромінених радіосистемами дистанційного зондування Землі з аерокосмічних носіїв та формалізації особливостей огляду підстильної поверхні у системі «РСА-РФ».

Ключові слова: теорія дистанційного зондування; формування радіозображень; отримання зображень з РСА; оброблення сигналів.

Павліков Володимир Володимирович – д-р техн. наук, проф., проректор з наукової роботи, Національний аерокосмічний університет ім. М. Є. Жуковського «Харківський авіаційний інститут», Харків, Україна.

Жила Семен Сергійович – д-р техн. наук, зав. кафедри аерокосмічних радіоелектронних систем, Національний аерокосмічний університет ім. М. Є. Жуковського «Харківський авіаційний інститут», Харків, Україна.

Поздняков Павло Васильович – канд. техн. наук, доц., Державний науково-дослідний інститут технологій кібербезпеки та захисту інформації Державної служби спеціального зв'язку та захисту інформації України, Київ, Україна.

Колесніков Денис Вікторович – д-р. філософії, доц. кафедри аерокосмічних радіоелектронних систем, Національний аерокосмічний університет ім. М. Є. Жуковського «Харківський авіаційний інститут», Харків, Україна.

Черепнін Гліб Сергійович – д-р філософії, доц. каф. аерокосмічних радіоелектронних систем, Національний аерокосмічний університет ім. М. Є. Жуковського «Харківський авіаційний інститут», Харків, Україна.

Шматко Олександр Олександрович – канд. техн. наук, нач. науково-дослідної частини, Національний аерокосмічний університет ім. М. Є. Жуковського «Харківський авіаційний інститут», Харків, Україна.

Одокієнко Олексій Володимирович – канд. техн. наук, декан факультету радіоелектроніки, комп'ютерних систем та інфокомунікацій, Національний аерокосмічний університет ім. М. Є. Жуковського «Харківський авіаційний інститут», Харків, Україна.

Малашта Павло Петрович – аспірант кафедри аерокосмічних радіоелектронних систем, Національний аерокосмічний університет ім. М. Є. Жуковського «Харківський авіаційний інститут», Харків, Україна.

Церне Едуард Олексійович – д-р. філософії, доц. кафедри аерокосмічних радіоелектронних систем, Національний аерокосмічний університет ім. М. Є. Жуковського «Харківський авіаційний інститут», Харків, Україна.

Volodymyr Pavlikov – D.Sc., Professor, Vice-Rector for Science, National Aerospace University "Kharkiv Aviation Institute", Kharkiv, Ukraine,
e-mail: v.pavlikov@khai.edu, ORCID: 0000-0002-6370-1758, Scopus Author ID: 23397933100.

Simeon Zhyla – D.Sc., Head of the Aerospace Radioelectronic Systems Department, National Aerospace University "Kharkiv Aviation Institute", Kharkiv, Ukraine,
e-mail: s.zhyla@khai.edu, ORCID: 0000-0003-2989-8988, Scopus Author ID: 57207914339.

Pavlo Pozdniakov – PhD, Associate Professor, State Scientific and Research Institute of Cybersecurity Technologies and Information Protection SSSCIP of Ukraine, Kyiv, Ukraine, e-mail: ictip@cip.gov.ua.

Denys Kolesnikov – PhD, Associate Professor at the Aerospace Radioelectronic Systems Department, National Aerospace University "Kharkiv Aviation Institute", Kharkiv, Ukraine,
e-mail: d.kolesnikov@khai.edu, ORCID: 0000-0002-0135-2695, Scopus Author ID: 57207915447.

Hlib Cherepnin – PhD, Associate Professor at the Aerospace Radioelectronic Systems Department, National Aerospace University "Kharkiv Aviation Institute", Kharkiv, Ukraine,
e-mail: g.cherepnin@khai.edu, ORCID: 0000-0003-1245-0933, Scopus Author ID: 57220835419.

Olexandr Shmatko – PhD, Head of the Scientific and Research Department, National Aerospace University "Kharkiv Aviation Institute", Kharkiv, Ukraine,
e-mail: o.shmatko@khai.edu, ORCID: 0000-0002-3236-0735, Scopus Author ID: 58198933300.

Oleksii Odokiienko – PhD, Dean of the Faculty of Radio Electronics, Computer Systems and Infocommunications, National Aerospace University "Kharkiv Aviation Institute", Kharkiv, Ukraine,
e-mail: o.odokiienko@khai.edu, ORCID: 0000-0002-5227-1000, Scopus Author ID: 56784405500.

Pavlo Malashta – PhD Student of the Aerospace Radioelectronic Systems Department, National Aerospace University "Kharkiv Aviation Institute", Kharkiv, Ukraine,
e-mail: p.p.malashta@khai.edu, ORCID: 0009-0000-2652-1507.

Eduard Tserne – PhD, Associate Professor at the Aerospace Radioelectronic Systems Department, National Aerospace University "Kharkiv Aviation Institute", Kharkiv, Ukraine,
e-mail: e.tserne@khai.edu, ORCID: 0000-0003-0709-2238, Scopus Author ID: 57218704755.